Molecular Neurobiology (2023) 60:3553–3567
https://doi.org/10.1007/s12035-023-03294-y

TR-FRET-Based Immunoassay to Measure Ataxin-2 as a Target Engagement Marker in Spinocerebellar Ataxia Type 2

Jessica Bux[1,2] · Nesli Ece Sen[3,4] · Isa-Maria Klink[1,2] · Stefan Hauser[5,6] · Matthis Synofzik[5,6] · Ludger Schöls[5,6] · Georg Auburger[3] · Olaf Riess[1,2,7] · Jeannette Hübener-Schmid[1,2]

Received: 11 October 2022 / Accepted: 22 February 2023 / Published online: 9 March 2023

Abstract

Spinocerebellar ataxia type 2 (SCA2) is an autosomal dominantly inherited neurodegenerative disease, which belongs to the trinucleotide repeat disease group with a CAG repeat expansion in exon 1 of the *ATXN2* gene resulting in an ataxin-2 protein with an expanded polyglutamine (polyQ)-stretch. The disease is late manifesting leading to early death. Today, therapeutic interventions to cure the disease or even to decelerate disease progression are not available yet. Furthermore, primary readout parameter for disease progression and therapeutic intervention studies are limited. Thus, there is an urgent need for quantifiable molecular biomarkers such as ataxin-2 becoming even more important due to numerous potential protein-lowering therapeutic intervention strategies. The aim of this study was to establish a sensitive technique to measure the amount of soluble polyQ-expanded ataxin-2 in human biofluids to evaluate ataxin-2 protein levels as prognostic and/or therapeutic biomarker in SCA2. Time-resolved fluorescence energy transfer (TR-FRET) was used to establish a polyQ-expanded ataxin-2-specific immunoassay. Two different ataxin-2 antibodies and two different polyQ-binding antibodies were validated in three different concentrations and tested in cellular and animal tissue as well as in human cell lines, comparing different buffer conditions to evaluate the best assay conditions. We established a TR-FRET-based immunoassay for soluble polyQ-expanded ataxin-2 and validated measurements in human cell lines including iPSC-derived cortical neurons. Additionally, our immunoassay was sensitive enough to monitor small ataxin-2 expression changes by siRNA or starvation treatment. We successfully established the first sensitive ataxin-2 immunoassay to measure specifically soluble polyQ-expanded ataxin-2 in human biomaterials.

Keywords Spinocerebellar ataxia type 2 · Ataxin-2 · Biomarker · Time-resolved fluorescence energy transfer · Target engagement

✉ Jeannette Hübener-Schmid
Jeannette.Huebener@med.uni-tuebingen.de

1 Institute of Medical Genetics and Applied Genomics, University of Tübingen, Tübingen, Germany

2 Centre for Rare Diseases, Medical Faculty, University of Tübingen, Tübingen, Germany

3 Experimental Neurology, Goethe University, Frankfurt am Main, Germany

4 Department of Molecular and Cellular Biology, Faculty of Sciences III, University of Geneva, Geneva, Switzerland

5 Department for Neurodegenerative Diseases and Hertie-Institute for Clinical Brain Research, University of Tübingen, Tübingen, Germany

6 German Center for Neurodegenerative Diseases (DZNE), Tübingen, Germany

7 NGS Competence Center Tübingen, Tübingen, Germany

Abbreviations

1C2-D2	PolyQ-specific antibody 1C2, D2 labeled
AD	Alzheimer's disease
ALS	Amyotrophic lateral sclerosis
Ataxin2mono-Tb	Monoclonal ATXN2 antibody, Tb labeled
Ataxin2poly-Tb	Polyclonal ATXN2 antibody, Tb labeled
ATXN2	Ataxin-2 (protein)
Ax	SCA2 patient
CN	iPSC-derived cortical neuron
Co	Control patient
CSF	Cerebrospinal fluid
DRPLA	Dentatorubral-pallidoluysian atrophy
ex	Expanded
FBS	Fetal bovine serum
FTD	Frontotemporal dementia

HBSS	Hanks' Balanced Salt Solution
HD	Huntington's disease
HEK	Human embryonic kidney
iPSC	Induced pluripotent stem cell
KI	Knock-in
LOD	Limit of detection
LOQ	Limit of quantification
Luc	Luciferase
MEF	Mouse embryonic fibroblast
MW1-D2	PolyQ-specific antibody MW1, D2 labeled
NfL	Neurofilament light
PBMC	Peripheral blood mononuclear cells
polyQ	Polyglutamine
Q	Glutamine
RT	Room temperature
SARA	Scale for the Assessment and Rating of Ataxia
SBMA	Spinal and bulbar muscular atrophy
SCA	Spinocerebellar Ataxia
SCA2	Spinocerebellar Ataxia Type 2
SEM	Standard error of the mean
SMC	Single-molecule counting
SNCA	α-synuclein
TPM	Transcript per million
TR-FRET	Time-resolved fluorescence energy transfer
TTR-FAP	Transthyretin familial amyloid polyneuropathy
WT	Wildtype

Introduction

Spinocerebellar ataxia type 2 (SCA2) is an autosomal dominantly inherited neurodegenerative disease which is caused by the expansion of the triplet CAG in exon 1 of the *ATXN2* gene localized on chromosome 12q24 [1, 2]. The triplet CAG encodes for the amino acid glutamine (Q) and therefore, SCA2 belongs to the group of polyglutamine (polyQ) expansion diseases like Huntington's disease (HD); SCA1, 3, 6, 7, 17; dentatorubral-pallidoluysian atrophy (DRPLA); and spinal and bulbar muscular atrophy (SBMA). Normal repeat length varies between 14 and 29 glutamines (most individuals have 22Q) [3], and intermediate length alleles (27–33Q) are associated with amyotrophic lateral sclerosis (ALS) [4] and a length of more than 32Q results in SCA2 [5], while most SCA2 patients show expanded repeats between 36 and 52, respectively [6, 7], and rare expansions beyond 800Q were observed [8].

For SCA2, mean age of onset is about 32 years. Age of onset, disease duration but also clinical manifestation show substantial variability. Key features include cerebellar ataxia and slowing of saccadic eye movements in variable combination with cerebellar dysarthria, dysphagia, peripheral neuropathy, and postural tremor. Degeneration of Purkinje cells in the cerebellum is the main neuropathological hallmark of SCA2 [7, 9–21].

The protein ataxin-2 (ATXN2) is predominantly localized in the cytosol [22] and is leading with disease progression to intranuclear inclusions in the brainstem [23] and to cytoplasmic "micro"aggregates in cerebellar Purkinje cells [24]. ATXN2 has a role in posttranscriptional RNA modification, quality control, and translation [25–29]. Under stress conditions, the expression and translation of ATXN2 is enhanced, and the protein relocalizes into stress granules [30].

So far, there is no curative therapy for SCA2 [31]. Clinical studies are difficult as primary readout parameters reflecting disease activity or key pathogenic processes are limited. Clinical scores like the Scale for the Assessment and Rating of Ataxia (SARA) are commonly used to monitor disease progression but show a high inter-rater and day-to-day variability [32]. Neurofilament light (NfL) is the best-established fluid biomarker for measuring neurodegeneration in several neurodegenerative diseases but with poor specificity [33]. For SCA2, NfL levels were associated with disease severity and cerebellar atrophy as well as get increased already before disease onset in pre-ataxic mutation carriers [34–36]. Another biofluid marker which shows potential as neurodegenerative marker in different neurological disorders including SCA2 is tau, a protein which promotes microtubule assembly and stability and is released under neuroaxonal damage. In SCA2, tau was significantly elevated in CSF compared to controls [37]. Additionally, imaging analyses showed olivopontocerebellar atrophy and pontine brainstem volume loss before disease onset and thalamus as well as parietal cortical atrophy at higher disease stages [38–40]. With the development of disease protein-lowering therapies like siRNA or antisense oligonucleotides (ASO) in polyQ diseases, the soluble disease protein itself represents a promising target-based molecular marker to measure protein lowering under therapies (target engagement). Therefore, for several polyQ diseases like HD [41–43] or SCA3 [44, 45], TR-FRET-based immunoassays for quantification of total and polyQ-expanded disease proteins, like huntingtin or ataxin-3, have been established. Additionally, to detect very low protein concentrations in peripheral blood or CSF, ultrasensitive single-molecule counting (SMC) immunoassays were validated [46, 47] and used as prognostic and/or therapeutic readout parameters. In SCA2, the disease protein ATXN2 could also represent a potential prognostic and/or therapeutic biomarker, as the amount of polyQ-expanded ATXN2 in, e.g., blood or CSF, may reflect the course of the disease and potential therapeutic success.

Intermediated repeat expansions in ATXN2 (27-32Qs) are viewed as a genetic risk factor, as they modulate the pathogenesis and the age at onset of several other neurodegenerative diseases including transthyretin familial amyloid polyneuropathy (TTR-FAP), frontotemporal dementia (FTD), Alzheimer´s disease (AD), corticobasal syndrome, ALS, and SCA3 [48–54]. Furthermore, CAA interruptions within the CAG repeat are claimed to have an influence on the pathogenesis and the phenotype of neurological diseases [48]. It is assumed that CAA interruptions are stabilizing the CAG repeat and therefore may explain why intermediated repeats are associated with, e.g., ALS and other neurological disorders but did not result in a mild type of SCA2 [55]. Whereas SCA2 patients demonstrate only an uninterrupted CAG repeat within ATXN2, a patient with corticobasal syndrome was reported which demonstrated 27/39 CAG repeats within ATXN2 with a CAG repeat interrupted by three (intermediated allele) or four (expanded allele) CAA motifs. This patient did not suffer from SCA2 [56]. Recently, a 9-bp duplication within ATXN2 was identified which led to significant decrease in the age at onset in both SCA3 and C9orf72-ALS [57].

Therefore, the establishment of sensitive immunoassays to determine total and polyQ-expanded ATXN2 in human biofluids is not only of interest for the rare disease SCA2 but also for other (rare) neurological disorders. In the current study, it was our aim to provide a first step for the development of sensitive immunoassays for the quantitative determination of soluble polyQ-expanded ATXN2 protein in patient-derived cell lines and mammalian biomaterials.

Materials and Methods

Ethical Use of Animals

All mice were maintained by animal care staff and veterinarians of the University of Frankfurt/Main Zentrale Forschungs-Einrichtung (ZFE). All procedures were performed according to the German Animal Welfare Act and the guidelines of the Federation of European Laboratory Animal Science Associations, based on European Union legislation (Directive 2010/63/EU). Animal experiments were approved by the local ethics committee (Regierungs-Präsidium Darmstadt V54-19c18-FK/1083).

Ethical Use of Human Tissue

All the work involving human tissue has been carried out in accordance with the Code of Ethics of the World Medical Association (Declaration of Helsinki) and with national legislation as well as our institutional guidelines. Experiments were approved by the local ethics committee (ethical vote Tübingen, 598/2011BO1 and 911/2019BO2).

Mouse and iPSC Sample Description

Different mouse tissues (liver, hemisphere, cerebellum) isolated from young (2.5–3 months) and old (14–18 months) knock-in mouse lines modeling SCA2, including *ATXN2*-CAG42 [58] and *Atxn2*-CAG100 knock-in mice [59], were used during the establishment of the assay conditions. The generation of mouse embryonic fibroblast (MEF) lines from *Atxn2*-CAG100 knock-in mice was reported before [59]. Human fibroblasts were isolated from skin biopsies of three SCA2 patients and three neurologically healthy controls after written informed consent. Fibroblasts were reprogrammed into induced pluripotent stem cells (iPSCs) as specified earlier [60] and differentiated into cortical neurons (CNs) as described before [61]. Specification of analyzed human cell lines are represented in Table 1. Human serum samples from four SCA2 patients and five neurologically healthy controls were isolated using serum preparation tubes (BD Biosciences, Heidelberg, Germany).

Cell Culture and Transfection

MEF and human embryonic kidney (HEK293T) cells were maintained in DMEM (Thermo Fisher Scientific, Waltham, USA) supplemented with 10% fetal bovine serum (FBS) and 1% antibiotics-antimycotics (both Thermo Fisher Scientific, Waltham, USA) at 5% CO_2 and 37 °C. For MEF, experiments were carried out only within the first 5 passages. Different ATXN2 plasmids including GFP-ATXN2-22Q/myc-ATXN2-22Q, GFP-ATXN2-79Q/myc-ATXN2-79Q, or GFP-empty/myc-empty as internal control were used for transfection experiments.

HEK293T cells were transfected with GFP or myc ATXN2 plasmids with different polyQ length (GFP-22Q/myc-22Q, GFP-79Q/myc-79Q, or GFP-empty/myc-empty as internal control) with Attractene transfection reagent (Qiagen, Hilden, Germany) using the traditional transfection

Table 1 Specification of human cell lines used in this study

Line	Number of iPSC clones	*ATXN2* CAG repeat length	Age at biopsy	Sex
Co-1	1	21/21	74 years	Male
Co-2	1	14/21	69 years	Female
Co-3	1	14/23	46 years	Female
Co-4	1	21/23	46 years	Male
Ax-1	2	23/36	31 years	Male
Ax-2	1	22/42	36 years	Female
Ax-3	1	22/38	45 years	Female

protocol. Shortly, 24 h before transfection, 400,000 HEK293T cells per well were seeded on a six-well tissue culture plate in DMEM medium. For transfection, 1.2 µg plasmid DNA, 100 µl OptiMEM (Thermo Fisher Scientific, Waltham, USA), and 4.5 µl Attractene Transfection Reagent were mixed, incubated for 15 min at room temperature (RT), and afterwards dropped carefully on the seeded cells. Seventy-two hours after transfection, HEK293T cells as well as MEF cells were harvested with DPBS (Thermo Fisher Scientific, Waltham, USA), centrifuged for 5 min at 300*g*, and directly lysed in RIPA buffer (50 mM Tris, pH 8.0, 150 mM NaCl, 0.1% SDS, 0.5% sodium deoxycholate, 1% IGEPAL) supplemented with cOmplete (EDTA-free) Protease Inhibitor (Roche, Mannheim, Germany) followed by incubation on ice for 30 min and vortexing every 10 min. For lysate preparation, the cell homogenates were centrifuged for 30 min at 4 °C and 16,100*g*. The Bradford protein assay was used to determine the total protein concentration [62].

Cell Culture Starvation and siRNA Experiments

For the starvation experiments, 400,000 HEK293T cells per well were seeded on a six-well tissue culture plate and transfected with ATXN2 GFP-22Q, GFP-79Q or GFP-empty as control, as described above.

Seventy-two hours after transfection, the medium was changed to Hanks' Balanced Salt Solution (Thermo Fisher Scientific, Waltham, USA) and incubated for either 0 h, 1 h, or 2 h, respectively. After incubation, cells were harvested as described.

For esiRNA experiments, knockdown of ATXN2 was achieved using endoribonuclease-prepared siRNA (esiRNA) directed against human ATXN2 (MISSION® esiRNA EHU104101, Sigma-Aldrich, Missouri, USA) or control esiRNA against *Renilla* luciferase (MISSION® esiRNA EHURLUC, Sigma-Aldrich, Missouri, USA). Four hundred thousand HEK293T cells per well were seeded on a six-well tissue culture plate. The transfection followed the traditional Attractene transfection protocol (Qiagen, Hilden, Germany) with 1.2 µg plasmid DNA (ATXN2 GFP-22Q, ATXN2 GFP-79Q or GFP-empty as control), 18 pmol esiRNA, and 4.5 µl Attractene Transfection Reagent. Seventy-two hours after transfection, cells were harvested with DPBS, centrifuged for 5 min at 300*g* and lysed in RIPA for 30 min on ice and vortexing every 10 min.

Isolation of Recombinant ATXN2

HEK293T cells (1.2×10^7) were seeded per 175 cm^2 cell culture dish. After 24 h, cells were transfected with 8 µg ATXN2 Myc-22Q or Myc-79Q constructs using polyethylenimine (PEI) transfection reagent (Polysciences, Warrintong, USA). Seventy-two hours after transfection, cells were harvested in M-Per Mammalian Protein Extraction Reagent (Thermo Fisher Scientific, Waltham, USA) followed by lysis of adherent mammalian cells and procedure for IP of Myc-tagged proteins using Pierce Anti-Myc Agarose as described in the instruction manual (Thermo Fisher Scientific, Waltham, USA). Recombinant proteins were eluted using Pierce IgG Elution buffer (Thermo Fisher Scientific, Waltham, USA).

Protein Extraction

For the establishment of the TR-FRET, mouse tissues and cells were homogenized in three different lysis buffers: RIPA buffer (50 mM Tris, pH 8.0, 150 mM NaCl, 0.1% SDS, 0.5% sodium deoxycholate, 1% IGEPAL), TES buffer (20 mM Tris, pH 7.5, 2 mM EDTA, 100 mM NaCl) supplemented with TNES buffer (50 mM Tris pH 7,5, 2 mM EDTA, 100 mM NaCl, 1% IGEPAL), or PBS buffer (DPBS (1×) Dulbecco's Phosphate-Buffered Saline with 1% Triton™ X-100). All buffers were supplemented with cOmplete (EDTA-free) Protease Inhibitor (Roche, Mannheim, Germany). For each buffer condition, 10 mg tissue or cells were homogenized mechanistically in 100 µl of the respective buffer using the VDI 12 homogenisator (VWR, Darmstadt, Germany). Afterwards, homogenates were incubated on ice for 30 min vortexing every 10 min. Homogenates were stored at − 80 °C for later TR-FRET analyzes. Part of the homogenates were centrifuged at 13 200*g* for 30 min. Lysates were transferred to new collection tubes supplemented with 10% glycerol and stored at − 80 °C for later western blot analyses. The Bradford protein assay was used to determine the total protein concentration from homogenates and lysates [62].

SDS-PAGE and Western Blot

Twenty to 30 µg of total protein from cell culture or mouse tissue lysates were supplemented with 4 × LDS sample buffer (1 M Tris pH 8.5, 2 mm EDTA, 8% LDS, 40% glycerol, 0.075% CBB G, 0.025% phenol red) in a ratio 3:1 and 0.1 M dithiothreitol. Samples were heat denatured for 10 min at 70 °C and afterwards, electrophoretically separated [63] using 8 to 10% Bis-Tris gels with the electrophoresis MOPS buffer (50 mM MOPS, 50 mM Tris pH 7.7, 0.1% SDS, 1 mM EDTA) at 100 V, 250 mA for 2–2.5 h. Proteins were blotted [64] on nitrocellulose membranes (Amersham Protran Premium 0.2 µm, GE Healthcare) using transfer buffer (25 mM Bicine, 25 mM Bis-Tris pH 7.2, 1 mM EDTA, 15% methanol) at 80 V and 250 mA for 1.5 h. After transfer, the membranes were blocked with 5% skim milk powder in Tris-buffered saline (TBS) for 1 h, washed with TBS-T (TBS with 0.1% Tween 20) and incubated overnight at 4 °C with the following primary antibodies diluted in TBS-T: ataxin-2 polyclonal antibody (1:1000,

21776-1-AP, rabbit, Proteintech Group, Rosemont, USA); mouse anti-β-actin monoclonal antibody (1:500, clone AC-15, Sigma-Aldrich, Darmstadt, Germany). Afterwards, membranes were washed with TBS-T and incubated at RT for 1 h with secondary IRDye antibodies goat anti-mouse 800CW or goat anti-rabbit 800CW (both 1:5000, Li-Cor Biotechnology GmbH, Bad Homburg, Germany), respectively. After washing with TBS-T, fluorescence signals were detected using the LI-COR ODYSSEY FC and quantified with Image Studio 4.0 software (both Li-Cor Biotechnology GmbH, Bad Homburg, Germany). All full western blot images are provided as supplementary information figure 3a-f.

TR-FRET

To establish a polyQ-expanded ATXN2 specific time resolved fluorescence energy transfer (TR-FRET)-based immunoassay, two different ATXN2 antibodies and two different polyQ-specific antibodies were compared. Therefore, the two ATXN2 specific antibodies ataxin-2 polyclonal antibody (21776-1-AP, Proteintech Group, Rosemont, USA) and purified mouse anti-ataxin-2 monoclonal antibody (AB_398900, Becton, Dickinson and Company, Sparks, USA) were labeled with the fluorophore Tb by the company CisBio Inc. (PerkinElmer, Waltham, USA). Additionally, the two polyQ-specific antibodies clone MW1 (AB 528290, Development Studies Hybridoma Bank, Iowa, USA), and clone 5TF1-1C2 (MAB1574, Sigma-Aldrich, Darmstadt, Germany) received the acceptor fluorophore D2 by the same company. For establishment of the TR-FRET-based immunoassay, the labeled antibodies were diluted in detection buffer (50 mM NaH_2PO_4, 400 mM NaF, 0.1% BSA, 0.05% Tween-20) in different concentrations (Tb-labeled antibodies: 0.3 ng, 0.5 ng, 1 ng and D2-labeled antibodies: 1 ng, 3 ng, 10 ng). Mouse tissue or cell culture homogenates were diluted to a total protein concentration of either 2 µg/µl or 1 µg/µl in one of the following buffers (RIPA, TES/TNES or PBS) supplemented with cOmplete (EDTA-free) Protease Inhibitor. Human serum samples were measured undiluted or diluted 1:2 or 1:4 with PBS supplement with cOmplete (EDTA-free) Protease Inhibitor, respectively. Five microliters per diluted sample was incubated in duplicates with 1 µl antibody-mix (Tb-antibody with D2-antibody, ratio 1:1) in a low-volume white ProxiPlate 384 TC Plus plate (PerkinElmer, Waltham, USA) for 24 h at 4 °C. Signals were detected at 620 nm and 665 nm with the Multimode Plate Reader Envision (PerkinElmer, Waltham, USA), and the ratio between 665/620 was normalized to the total protein concentration and over the background signal (deltaF).

Statistical Analysis

The program GraphPad Prism 8 (GraphPad Software Inc., San Diego, USA) was used for the statistical evaluation of all data and for data visualization. Limit of detection (LOD) and quantification (LOQ) were calculated using GraphPad Prism software with a nonlinear regression model using a two-site binding saturation curve fit (including specific and background signal). The LOD is defined as the lowest concentration giving a signal greater than the background signal (above 3 standard deviations). The LOQ is defined as the lowest concentration giving a signal greater than the background signal (+ 10 standard deviations).

Normality of the datasets was evaluated by Shapiro-Wilk test. Due to the non-normally distributed data, the non-parametric Mann-Whitney *U* test was used to compare the different groups. *P*-values with less than 0.05 were considered statistically significant with $*p < 0.05$, $**p < 0.01$, and $***p < 0.001$. All values are shown as mean ± standard error of the mean, SEM.

Results

Establishment of Antibody Combination and Concentration

To establish a TR-FRET-based immunoassay to quantify specifically soluble polyQ-expanded ATXN2 protein, two different Tb-labeled ATXN2 specific antibodies (polyclonal ATXN2 antibody (ataxin2poly-Tb, aa 251-600) and monoclonal ATXN2 antibody (Ataxin2mono-Tb, aa 713-904)) as well as two different D2-labeled polyQ-specific antibodies (MW1-D2 (≥ 15Q) and 1C2-D2 (≥ 37Q)) were tested in combination with each other, each at three different concentrations (for Tb 0.3 ng, 0.5 ng and 1 ng/µl, for D2 1 ng, 3 ng, and 10 ng/µl) (schematic representation in Fig. 1a). If both antibodies bind specifically and in close proximity, an energy transfer takes place between the donor (Tb) and the acceptor (D2). The measured signal is proportional to the ATXN2 protein concentration of the tested sample and needs to be normalized to the total protein concentration and over the background signal. To evaluate the different antibody combinations, liver homogenates from *Atxn2*-CAG100 knock-in mice [59] (blue; KI) compared to wildtype mice (red; WT) and homogenates of MEF from *Atxn2*-CAG100 knock-in mice [59] compared to wildtype mice were generated in RIPA buffer. For the antibody combination ataxin2poly-Tb × MW1-D2, the best discrimination between WT and KI was achieved with the concentration of ataxin2poly-Tb 0.3 ng/µl × MW1-D2 3 ng/µl (labeled in green, Fig. 1b). Antibody combination ataxin2poly-Tb x

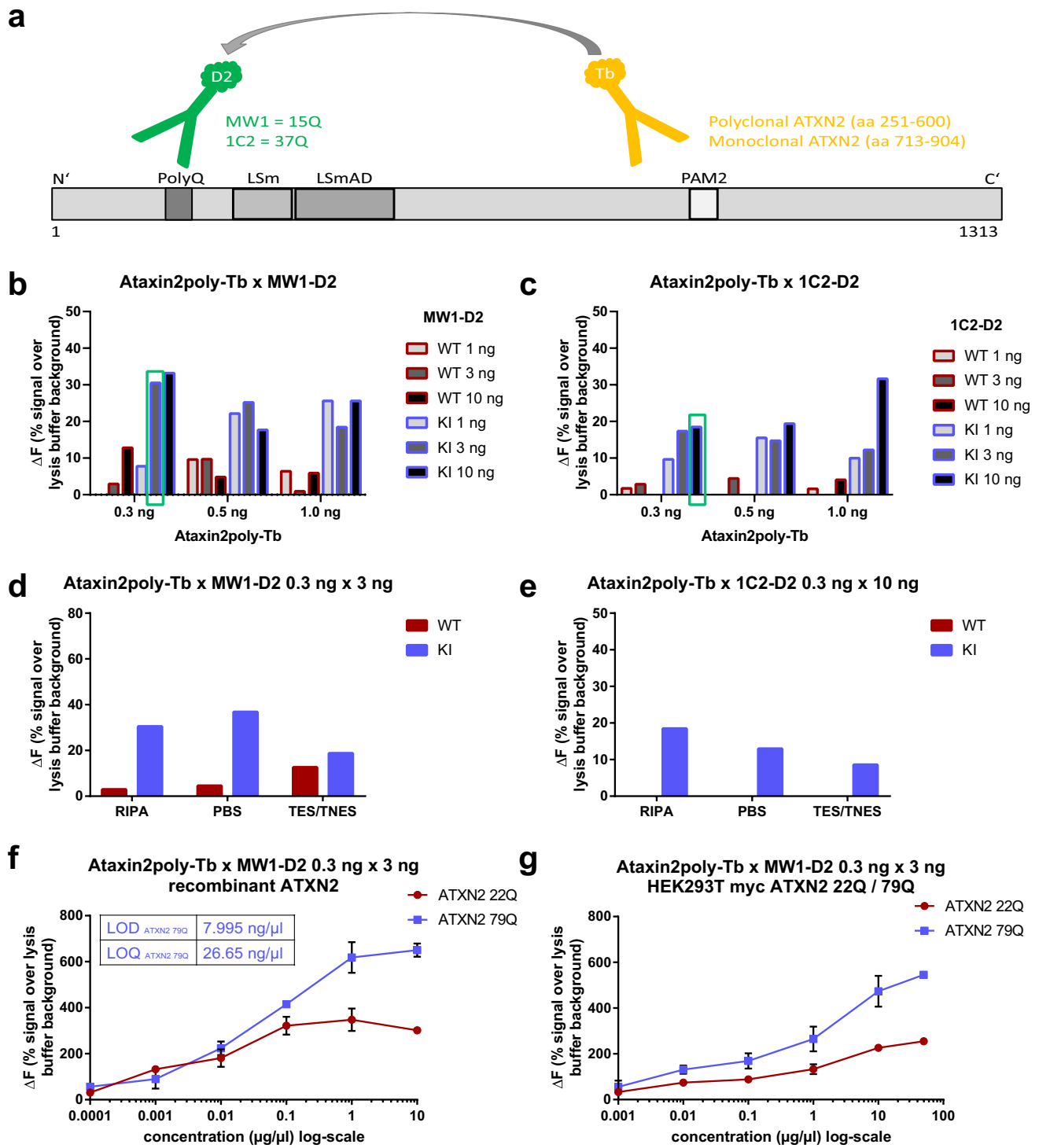

1C2-D2 showed the best discrimination between WT and KI with the concentration of ataxin2poly-Tb 0.3 ng/µl × 1C2-D2 10 ng/µl (labeled in green, Fig. 1c). Evaluation of MW1-D2 or 1C2-D2 in combination with the monoclonal ATXN2 antibody (Ataxin2mono-Tb) showed the best discrimination between WT and KI at the concentration of Ataxin2mono-Tb 0.5 ng/µl × MW1-D2 3 ng/µl (labeled in green, supplementary information figure 1a) or with Ataxin2mono-Tb 0.5 ng/µl × 1C2-D2 10 ng/µl (labeled in green, supplementary information figure 1b). In general, TR-FRET signals were lower when using the monoclonal ATXN2 antibody compared to the polyclonal ATXN2 antibody.

◂**Fig. 1** Establishment of a polyQ-expanded ATXN2 TR-FRET-based immunoassay. **a** Schematic illustration of the functional mechanism of a TR-FRET-based immunoassay to detect polyQ-expanded ATXN2. The ATXN2 protein with its four most important domains (PolyQ, LSm, LSmAD and PAM2) is shown to visualize the binding sites of the tested antibodies. Antibodies used as donor were labeled with the luminophore terbium cryptate (Tb) and the acceptor antibodies with the luminophore D2. Two D2-labeled antibodies (MW1-D2 and 1C2-D2) and two ATXN2-specific antibodies (ataxin2poly-Tb and Ataxin2mono-Tb) were tested. **b**, **c** Combination of the antibodies ataxin2poly-Tb and MW1-D2 (**b**) or ataxin2poly-Tb and 1C2-D2 (**c**) each in three different concentrations: ataxin2poly-Tb with 0.3 ng, 0.5 ng and 1 ng/µl, MW1- D2 or 1C2-D2 with 1 ng, 3 ng, and 10 ng/µl. Conduction of the TR-FRET measurement with homogenates from wildtype mouse liver (red; WT) and Atxn2-CAG100 knock-in mouse liver (blue; KI) lysed in RIPA buffer, using a total protein concentration of 1 µg/µl. The highest discrimination between WT and KI (green box) was achieved with the concentrations of ataxin2poly-Tb 0.3 ng/µl × MW1-D2 3 ng/µl (**b**) and ataxin2poly-Tb 0.3 ng/µl x 1C2-D2 10 ng/µl (**c**). **d**, **e** Comparison of three different lysis buffers including RIPA, PBS, and TES/TNES. TR-FRET measurement with homogenates from wildtype mouse liver (red; WT) and Atxn2-CAG100 knock-in mouse liver (blue; KI) in the established antibody concentrations: ataxin2poly-Tb 0.3 ng/µl × MW1-D2 3 ng/µl (**d**) and ataxin2poly-Tb 0.3 ng/µl × 1C2-D2 10 ng/µl (**e**). **f**, **g** Detection of purified recombinant ATXN2 proteins (**f**) or protein homogenates overexpressing ATXN2 of various lengths (**g**) with the antibody combination ataxin2poly-Tb 0.3 ng/µl × MW1-D2 3 ng/µl showed specificity for polyQ-expanded ATXN2 (ATXN2 79Q) over normal ATXN2 (ATXN2 22Q). The assay's limit of detection (LOD) was defined as the concentration corresponding to the signal 3 SDs above the lysis buffer background (zero calibrator) and upper limit of quantification (LOQ) as the concentration corresponding to the signal 10 SDs above the lysis buffer background. LOD = 7.995 ng/µl and LOQ = 26.65 ng/µl for recombinant ATXN2 79Q

Establishment of Buffer Conditions

To optimize lysis buffer conditions to best detergent (e.g., TritonX, Igepal) and ionic strength (NaCl concentration), three often used lysis buffers (RIPA, PBS and TES/TNES) were compared (Fig. 1d, e) for the antibody combinations ataxin2poly-Tb x MW1-D2 (Fig. 1d) and ataxin2poly-Tb × 1C2-D2 (Fig. 1e), each at the best antibody concentrations as established for RIPA buffer in Fig. 1b, c, for PBS buffer in supplementary information figures 1c+d and for TES/TNES buffer in supplementary information figures 1e+f. Protein homogenates in RIPA buffer reached the highest signals and the best discrimination between WT and KI. Therefore, all further experiments were carried out in RIPA buffer.

Establishment of Protein Amount

After establishing the antibody combinations, concentrations, and buffer conditions, recombinant ATXN2 isolated from HEK293T cells using Myc-tagged ATXN2 constructs and anti-c-myc agarose were used to prepare a standard curve with a concentration range from 10 to 0.0001 µg/µl recombinant ATXN2 protein with either 22Q or 79Q. TR-FRET immunoassay validation demonstrated a higher specificity for polyQ-expanded ATXN2 (79Q) over normal ATXN2 (22Q, Fig. 1f). Determination of LOD (limit of detection, 7.995 ng/µl) and LOQ (limit of quantification, 26.65 ng/µl) showed a linear detection threshold from 1 ng to 1 µg of recombinant ATXN2 79Q (Fig. 1f). Additionally, a standard curve generated using homogenates from HEK293T cells overexpressing Myc-22Q (red; 22Q) or Myc-79Q (blue; 79Q) revealed also a higher specificity for polyQ-expanded ATXN2 over normal ATXN2 as well as a linear detection range of 10 ng to 10 µg whole protein amount (Fig. 1g). To determine the best total protein concentration for further TR-FRET measurements, MEF homogenates including 2 or 1 µg/µl whole protein concentration isolated from *Atxn2*-CAG100 knock-in mice (blue; KI) or wild-type controls (red; WT) were evaluated (supplementary information figure 2a). Additionally, homogenates (2 or 1 µg/µl) from HEK293T cells transfected with myc ATXN2 plasmids including myc-22Q (red; 22Q) and myc-79Q (blue; 79Q) or empty plasmid (black; Ø) (supplementary information figure 2b) including 2 µg/µl or 1 µg/µl whole protein concentration were used. Samples were lysed in RIPA buffer and measured with the antibody combination ataxin2poly 0.3 ng/µl × MW1-D2 3 ng/µl. Results for the antibody combination Ataxin2mono-Tb 0.5 ng/µl × MW1-D2 3 ng/µl are also shown in the supplement (supplementary information figures 2c+d). Overall, measurements demonstrated that a lower total protein concentration of 1 µg/µl showed higher polyQ-expanded ATXN2-specific signals and a better discrimination between WT and KI samples.

In summary, the polyclonal ATXN2 antibody ataxin2poly-Tb discriminated better between ATXN2 WT and KI samples in comparison to the monoclonal antibody Ataxin-2mono-Tb. Therefore, further experiments were performed either in the combination ataxin2poly-Tb x MW1-D2 with the antibody concentration 0.3 ng/µl × 3 ng/µl or in the combination ataxin2poly-Tb x 1C2-D2 with antibody concentration of 0.3 ng/µl × 10 ng/µl. Additionally, RIPA buffer and a total protein concentration of 1 µg/µl were used in all further measurements.

SCA2 Specificity

As mentioned before, SCA2 belongs to the group of polyQ diseases including SCA1, 3, 6, 7, HD, DRPLA, and SBMA. In each of these diseases, neurodegeneration is mainly triggered by translation of disease proteins with an elongated polyQ region that can potentially be detected by the polyQ-specific antibodies MW1 and 1C2. For the development of an immunoassay to quantify soluble polyQ-expanded protein ATXN2 in human biomaterials, it is therefore essential to demonstrate that no other polyQ proteins are detectable. For that reason, we performed a specificity experiment including

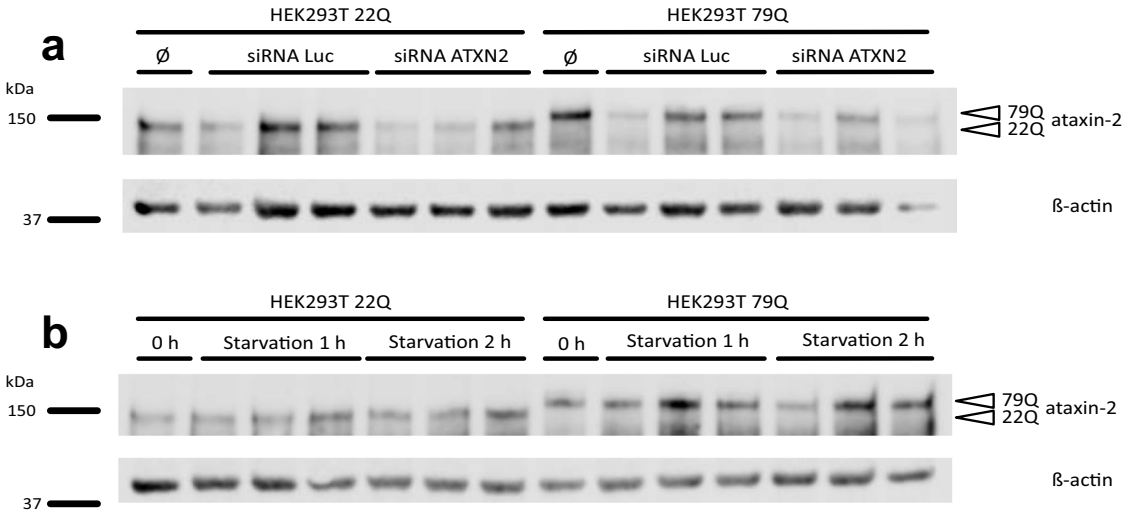
a
HEK293T 22Q
HEK293T 79Q
Ø
siRNA Luc
siRNA ATXN2
kDa
150
37
79Q
22Q
ataxin-2
ß-actin
b
HEK293T 22Q
HEK293T 79Q
0 h
Starvation 1 h
Starvation 2 h
kDa
150
37
79Q
22Q
ataxin-2
ß-actin

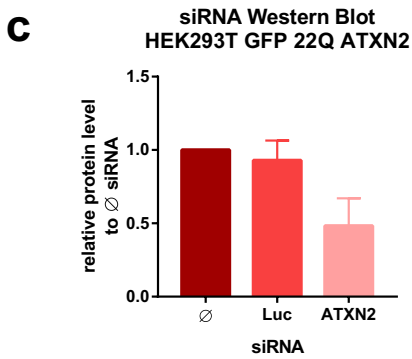
c
siRNA Western Blot
HEK293T GFP 22Q ATXN2
relative protein level to ∅ siRNA
1.5
1.0
0.5
0.0
∅
Luc
ATXN2
siRNA

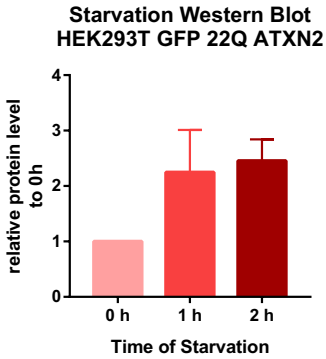
d
Starvation Western Blot
HEK293T GFP 22Q ATXN2
relative protein level to 0h
4
3
2
1
0
0 h
1 h
2 h
Time of Starvation

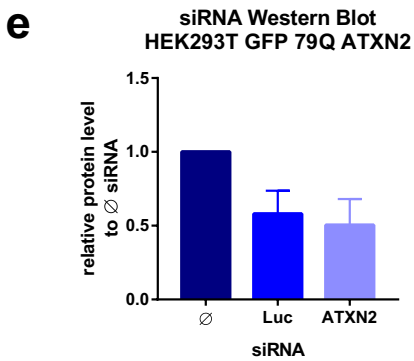
e
siRNA Western Blot
HEK293T GFP 79Q ATXN2
relative protein level to ∅ siRNA
1.5
1.0
0.5
0.0
∅
Luc
ATXN2
siRNA

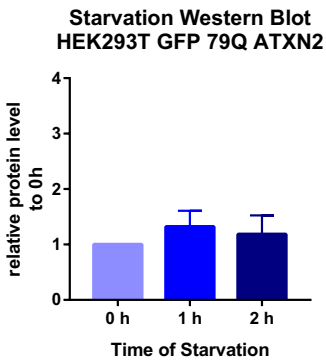
f
Starvation Western Blot
HEK293T GFP 79Q ATXN2
relative protein level to 0h
4
3
2
1
0
0 h
1 h
2 h
Time of Starvation

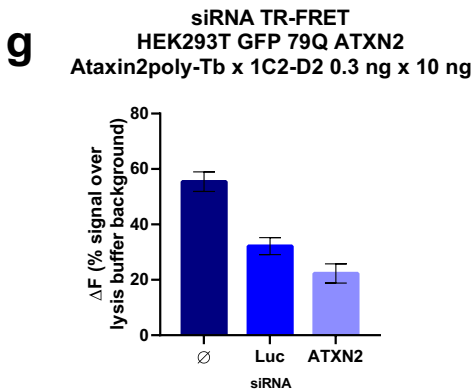
g
siRNA TR-FRET
HEK293T GFP 79Q ATXN2
Ataxin2poly-Tb x 1C2-D2 0.3 ng x 10 ng
ΔF (% signal over lysis buffer background)
80
60
40
20
0
∅
Luc
ATXN2
siRNA

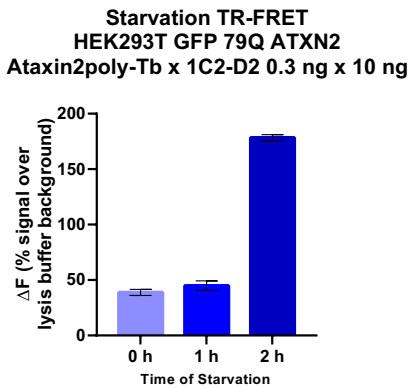
h
Starvation TR-FRET
HEK293T GFP 79Q ATXN2
Ataxin2poly-Tb x 1C2-D2 0.3 ng x 10 ng
ΔF (% signal over lysis buffer background)
200
150
100
50
0
0 h
1 h
2 h
Time of Starvation

◂**Fig. 2** siRNA and starvation experiments demonstrated that the TR-FRET-based immunoassay detects small changes in ATXN2 expression levels. To lower ATXN2 expression, HEK293T cells were transfected with GFP ATXN2 plasmids with 22Q or 79Q and treated either with ATXN2 siRNA (ATXN2), luciferase siRNA (Luc) as a control or without siRNA (Ø) (siRNA experiments). Additionally, GFP ATXN2 transfected HEK293T cells were incubated in HBSS for 0, 1, or 2 h to induce starvation, and therefore, ATXN2 upregulation **a**, **b** Western blot of siRNA experiments (**a**) and western blot of starvation experiments (**b**) using the polyclonal ataxin2poly antibody detected the ATXN2 protein at 150 kDa. β-actin is shown as loading control. (Western Blot analysis with 30 µg of total protein and 8% Bis-Tris gel) **c**–**f** Western blot quantification of ATXN2 expression after lowering by siRNA (**c**, **e**) or ATXN2 increased expression by starvation (**d**, **f**). The bars show the relative protein levels compared to treatment without siRNA (Ø) or 0 h of starvation, respectively. **g**, **h** TR-FRET analysis of the siRNA and starvation experiments using the antibody combination ataxin2poly-Tb 0.3 ng/µl × MW1-D2 10 ng/µl, diluted in RIPA buffer.

cerebellar homogenates from three wildtype controls and SCA2, SCA3, SCA17, and HD mouse models. The antibody combinations ataxin2poly-Tb 0.3 ng/µl × MW1-D2 3 ng/µl and ataxin2poly-Tb 0.3 ng/µl × 1C2-D2 10 ng/µl specifically measured polyQ-expanded disease protein only in the SCA2 samples (supplementary information figures 2e+f). As observed before, ATXN2 values were higher if measured with ataxin2poly-Tb × MW1-D2, but demonstrated also low background signals in controls and in other polyQ diseases.

Detection of Small Changes in ATXN2 Expression Levels Using siRNA and Starvation Experiments

As the primary reason to develop an immunoassay is to monitor therapeutic studies, the assay should be able to detect even small protein changes. Therefore, we downregulated ATXN2 expression in HEK293T cells using siRNA and increased polyQ-expanded ATXN2 levels by starvation experiments. For downregulation, HEK293T cells were transfected with GFP ATXN2 plasmids expressing 22Q or 79Q and treated with either ATXN2 siRNA (ATXN2), or as control reference with luciferase siRNA (Luc), or without siRNA (Ø, untreated). For starvation experiments, HEK293T cells transfected with GFP ATXN2 plasmids expressing 22Q or 79Q were grown in HBSS medium for 1 or 2 h to induce starvation. Western blot analyses detected the ATXN2 protein at 150 kDa using the polyclonal ataxin2poly antibody (Fig. 2a, b). Quantification of the ATXN2 22Q or 79Q protein expression under ATXN2 siRNA treatment revealed a slight downregulation compared to untreated or luciferase siRNA-treated cells (Fig. 2c, e). Additionally, inducing starvation revealed increased ATXN2 expression over time (Fig. 2d, f). Measuring the same samples as analyzed by western blot with the TR-FRET immunoassay revealed a clear downregulation of ATXN2 after ATXN2 siRNA treatment (Fig. 2g). The TR-FRET immunoassay analysis of the starvation experiments with 0, 1, or 2 h of starvation in HBSS medium detected an upregulation after 2 h of starvation using the antibody combination ataxin2poly-Tb 0.3 ng/µl × 1C2-D2 10 ng/µl (Fig. 2h).

ATXN2 Protein Level in Human Material

To assess if the developed immunoassay also measures human soluble polyQ-expanded ATXN2 specifically in human cell lines, different human cell lines including human fibroblasts (Fig. 3a) from SCA2 patients $n = 3$ (red; F-AX) and controls $n = 4$ (blue; F-Co), human iPSCs (Fig. 3b) from SCA2 patients $n = 4$ (red; iPSC-AX) and healthy controls $n = 4$ (blue; iPSC-Co), and human CNs (Fig. 3c) from SCA2 patients $n = 2$ (red; iCN-AX) and healthy controls $n = 4$ (blue; CN-Co) were diluted in RIPA buffer and tested with a total protein concentration of 1 µg/µl with the antibody combination ataxin2poly-Tb 0.3 ng/µl × MW1-D2 3 ng/µl. Our data showed that the newly developed TR-FRET immunoassay is capable to detect specifically soluble polyQ-expanded ATXN2 in patient-derived SCA2 biomaterials compared to respective controls. Western blot analyses confirmed ATXN2 expression in different cell lines (supplementary information figure 2g). Additionally, to determine if the established ATXN2 immunoassay is sensitive enough to measure ATXN2 protein levels in human biofluids, serum samples from 4 SCA2 mutation carrier as well as 5 neurologically healthy controls were analyzed using the antibody combination ataxin2poly-Tb 0.3 ng/µl × MW1-D2 3 ng/µl. Undiluted and 1:2 and 1:4 diluted serum samples were determined, and all measurements revealed lower protein expression values as calculated by the LOQ in both healthy controls and SCA2 patients (Fig. 3d).

Discussion

In this study, we developed the first sensitive TR-FRET-based immunoassay to measure the soluble polyQ-expanded protein ATXN2 in cellular and animal models as well as human neuronal cell culture.

There is currently no curative therapy for the trinucleotide repeat disease SCA2. One main reason for this is the lack of easily accessible, objective, and sensitive outcome parameters to track disease progression but also the lack of effective molecular target treatments. Unfortunately, clinical read outs such as the Scale for the Assessment and Rating of Ataxia (SARA) need long observation periods due to slow disease progression, show substantial day to day variability and inter-rater differences and rare prone to unspecific changes, e.g., due to injuries. For that reason, molecular markers that respond quickly to therapeutics and are readily detectable in biomaterials such as CSF or

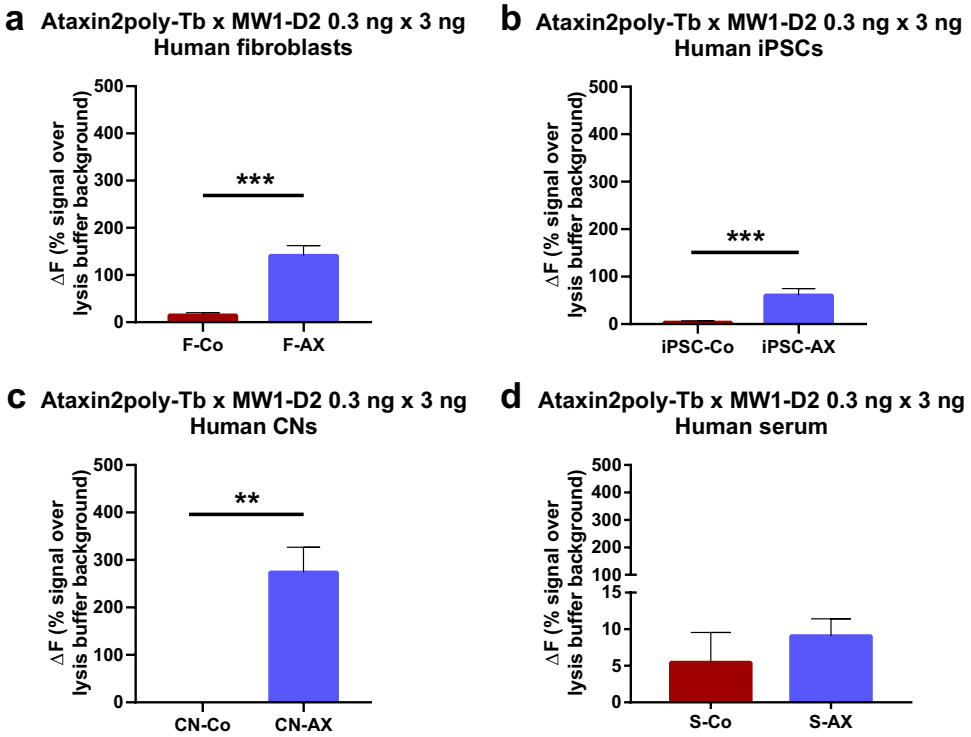

Fig. 3 TR-FRET analysis in human cell culture materials. **a** Determination of polyQ-expanded ATXN2 by TR-FRET-based immunoassay in homogenates of human fibroblasts isolated from SCA2 patients $n = 3$ (red; F-AX) and healthy controls $n = 4$ (blue; F-Co). **b** Homogenates of human iPSCs from SCA2 patients $n = 4$ (red; iPSC-AX) compared to $n = 4$ healthy controls (blue; iPSC-Co). **c** Homogenates of human CNs from SCA2 patients $n = 2$ (red; CN-AX) and healthy controls $n = 4$ (blue; CN-Co). **d** Human serum from SCA2 patients $n = 4$ (red; S-AX) compared to $n = 5$ healthy controls (blue; S-Co). All samples (except serum samples) were diluted in RIPA buffer, evaluated with a total protein concentration of 1 µg/µl and analyzed using the antibody combination ataxin2poly-Tb 0.3 ng/µl × MW1-D2 3 ng/µl. $^{**}P \leq 0.01$; $^{***}P \leq 0.001$

peripheral blood are of major importance for monitoring on-target effects for upcoming clinical trials. Recently, it has been shown that the protein tau has increased levels in CSF of SCA2 patients [37], and the protein neurofilament light (NfL) chain is suitable to indicate axonal degeneration in many neurodegenerative diseases, including SCA2 [34, 65]. Therapeutic strategies that reduce specifically polyQ-expanded protein levels are currently being applied to slow or stop disease progression in polyQ diseases like SCA1 [66, 67], SCA2 [68], HD [69, 70], and SCA3 [71–74]. Therefore, the disease proteins itself could serve as an excellent and primary potential therapeutic biomarker to monitor disease protein lowering by, e.g., antisense oligonucleotides. In HD [41–43] and SCA3 [44, 45], immunoassays based on the TR-FRET technology were already established to quantify the respective disease protein in human leukocytes, mononuclear cells (PBMCs), or human tissue samples. Later, the TR-FRET-based immunoassays were further developed into ultra-sensitive single-molecule counting (SMC) immunoassays in order to be able to quantify fmol protein amounts in CSF and peripheral blood of HD and SCA3 mutation carrier, too [46, 47]. Following its successful establishment in HD and SCA3, the soluble polyQ-expanded ATXN2 protein should also be validated as potential prognostic and therapeutic biomarker in SCA2.

To establish a new TR-FRET-based immunoassay for ATXN2, two antibodies which bind specifically to the disease protein are required. As shown for HD and SCA3, specific detection of the polyQ-expanded disease protein can be achieved by using one polyQ-specific antibody, like MW1. In our study, two different polyQ-specific antibodies were tested as acceptor antibodies: MW1 and 1C2. Importantly, both polyQ-specific antibodies are shown to have similar binding characteristics, which display similar binding properties with polyQ of various lengths [75]. To achieve SCA2 specificity, two ATXN2-specific antibodies were tested as donor antibody including a polyclonal ATXN2 antibody and a monoclonal ATXN2 antibody. Determination of best antibody pair and conditions revealed better results for the polyclonal ATXN2 antibody in combination with the polyQ-specific antibodies MW1 and 1C2. Following further optimizations, all biomaterials were subsequently lysed in RIPA buffer, biomaterial prediluted to a total protein concentration

of 1 µg/µl, and measurements performed after an incubation of biomaterial to antibody mixture for 24 h at 4 °C.

Since the polyQ-specific antibodies MW1 or 1C2 can also detect other proteins with an expanded polyQ region, we proved that the newly established ATXN2 immunoassay quantifies specifically the soluble polyQ-expanded ATXN2 protein. As shown already similarly for HD and SCA3, our newly established ATXN2 immunoassay specifically quantifies soluble polyQ-expanded ATXN2 if the polyQ-specific antibody MW1 is combined with an ATXN2-specific donor antibody [44].

In order to use the protein ATXN2 as a molecular readout parameter for disease progression and potentially in clinical trials which aim to reduce specifically the disease protein ("protein lowering therapies"), the immunoassay must be able to detect small protein changes. Therefore, down- and upregulated ATXN2 using siRNA and starvation experiments were performed and demonstrated that the polyQ-expanded ATXN2 immunoassay can reliably detect small protein changes.

To demonstrate target engagement in future trials that aim at silencing SCA disease genes, the availability of sensitive immunoassays to measure the concentration of polyQ-expanded disease proteins like ATXN2 in body fluids is mandatory [76]. Therefore, we confirmed that the new TR-FRET-based immunoassay is able to measure polyQ-expanded ATXN2 in human biomaterials like patient-derived cell lines including human fibroblasts, induced pluripotent stem cells, and iPSC-derived cortical neurons. Importantly, in all patient-derived cell lines, the immunoassay perfectly discriminated between SCA2 patients and healthy controls. However, the aim is to adapt the immunoassay to human biomaterials like cerebrospinal fluid (CSF) or peripheral blood. Unfortunately, first measurements in human SCA2 patient serum samples revealed that the level of expanded ATXN2 is lower as the determined immunoassay LOQ and therefore not high enough for evaluation with the newly developed TR-FRET-based immunoassay. As known for HD and SCA3, significantly lower concentrations of respective disease proteins are presumably present in the CSF or in peripheral blood [46, 47]. ATXN2 is a ubiquitous expressed protein, with high mRNA expression in all brain areas (e.g., cerebellum 33.10 TPM, transcript per million), but also hearth (11 TPM), kidney (10.28 TPM), lung (24.26 TPM), liver (8.950 TPM), and cultured fibroblasts with 15.98 TPM (https://gtexportal.org/home/gene/ENSG00000204842.14, [77]). The lowest expression is demonstrated for whole blood with 4.048 TPM, which explains why the polyQ-expanded ATXN2 immunoassay can measure successfully in patient-derived cell lines (cultured fibroblasts, 15.86 TPM) but not in serum isolated from whole blood (4.048 TPM) (https://gtexportal.org/home/gene/ENSG00000204842.14, [77]). ATXN2 is shown to increase to nutrient and trophic stress in a mTOR-signaling–dependent manner [78]. Therefore, it could be an option to perform a "fasting blood test" (no eat and drink for at least 8 h before blood take) to increase ATXN2 expression in whole blood and therefore may be able to increase ATXN2 expression to a measurable level by the newly developed TR-FRET-based assay.

Additionally, with the successfully established polyQ-expanded ATXN2 TR-FRET-based immunoassay, we have now the tool available to adapt the assay to an ultrasensitive platform like SMC or SIMOA in the future. As shown for HD and SCA3 that is important, because of very low–soluble protein levels in CSF, peripheral blood including serum and plasma [46, 47]. On mRNA level, HTT (huntingtin, 5.990 TPM), ATXN2 (4.048 TPM), and ATXN3 (0.8812 TPM) show only very low expression in whole blood compared to α-synuclein (SNCA) which demonstrate a high expression of 33.48 TPM (https://gtexportal.org/home/gene/ENSG00000204842.14, [77]). In line with that, no TR-FRET for measurements in whole blood or CSF could be established for HTT, ATXN3, or ATXN2 but showed positive results for SNCA [41–45, 79].

As indicated, the new ATXN2 immunoassay is with an assay range of around 1 ng to 10 µg more sensitive as other known techniques to determine protein expression including western blot analyses. But as most techniques, also this kind of immunoassay show some limitations including ran-translation [80], post-translational protein modifications [81], but also ATXN2 alternative splicing variants [82] or genomic mutations [48, 57, 83], which may interfere with the antibody binding sites. ATXN2 is shown to modulate different neurodegenerative diseases like ALS or SCA3 by intermediate repeat length [48]. Both, MW1 and 1C2 polyQ-specific antibodies, are characterized to bind glutamines of different length starting with 11Q but demonstrated higher affinity to longer repeats, because the number of epitopes is increasing with polyQ length (e.g., in the case of MW1, it increases from 13 epitopes in 22Q to 32 epitopes in 41Q) [75]. For SCA3 and HD, established immunoassays using the MW1 antibody results in the specific measurement of soluble polyQ-expanded disease protein and not determine controls with intermediated repeat length [46, 47]. To test that fact also for the newly developed soluble polyQ-expanded immunoassay ATXN2, we analyzed 5 PBMC samples from individuals with intermediated repeat length of 27 to 30 glutamines compared to individuals with 22Q. The measurements revealed lower signals as the determined immunoassay LOQ in both genotypes (data not shown) and might be explained by the fact that the multiplicity of epitopes of the polyQ-specific antibodies, combined with the possibility of several antigen-binding domain interacting

simultaneously on longer polyQ, constitute an unusually complex interaction. Therefore, conditions are present to detect only the longer polyQ, even when similar quantities of short and long polyQ are present [75].

In summary, we described the first ATXN2 immunoassay to measure specifically soluble polyQ-expanded ATXN2 in cellular and animal tissue as well as in human cell lines. Further validation in human biomaterials like CSF, peripheral blood, or PBMCs, including blood take under fasting conditions and correlation to clinical data, is needed to confirm polyQ-expanded ataxin-2 as new important molecular readout parameter in further patient-based studies.

Supplementary Information The online version contains supplementary material available at https://doi.org/10.1007/s12035-023-03294-y.

Acknowledgements We are grateful to Marilena Lauerer and Sabrina Beer for excellent technical assistance.

Author Contribution All the authors contributed to the study conception and design especially done by Olaf Riess, Jeannette Hübener-Schmid, and Jessica Bux. Material preparation, data collection, and analysis were performed by Jessica Bux and Isa-Maria Klink. Nesli Ece Sen, Stefan Hauser, Matthis Synofzik, Ludger Schöls, and Georg Auburger provided resources and prepared biomaterial for this study. The first draft of the manuscript was written by Jessica Bux and Jeannette Hübener-Schmid, and all the authors commented on previous versions of the manuscript. All the authors read and approved the final manuscript.

Funding Open Access funding enabled and organized by Projekt DEAL. This work was supported by "Interdisziplinäres Promotionskolleg Medizin", University of Tübingen (2020-2).

Data Availability All data generated during this study are included in this article or are available on reasonable request from the corresponding author.

Declarations

Ethics Approval Ethical use of animals: All mice were maintained by animal care staff and veterinarians of the University of Frankfurt/Main Zentrale Forschungs-Einrichtung (ZFE). All procedures were performed according to the German Animal Welfare Act and the guidelines of the Federation of European Laboratory Animal Science Associations, based on European Union legislation (Directive 2010/63/EU). Animal experiments were approved by the local ethics committee (Regierungs-Präsidium Darmstadt V54-19c18-FK/1083).

Ethical use of human tissue: All the work involving human tissue has been carried out in accordance with the Code of Ethics of the World Medical Association (Declaration of Helsinki) and with national legislation as well as our institutional guidelines. Experiments were approved by the local ethics committee (ethical vote Tübingen, 598/2011BO1 and 911/2019BO2).

Consent to Participate All patients gave written informed consent before enrollment.

Consent for Publication All study participants agreed in publication of the data with the informed consent.

Competing Interests The authors declare no competing interests.

References

1. Sanpei K, Takano H, Igarashi S, Sato T et al (1996) Identification of the spinocerebellar ataxia type 2 gene using a direct identification of repeat expansion and cloning technique. DIRECT. Nat Genet 14(3):277–284. https://doi.org/10.1038/ng1196-277
2. Gispert S, Twells R, Orozco G, Brice A et al (1993) Chromosomal assignment of the second locus for autosomal dominant cerebellar ataxia (SCA2) to chromosome 12q23-24.1. Nat Genet 4(3):295–299. https://doi.org/10.1038/ng0793-295
3. Sobczak K, Krzyzosiak WJ (2004) Patterns of CAG repeat interruptions in SCA1 and SCA2 genes in relation to repeat instability. Hum Mutat 24(3):236–247. https://doi.org/10.1002/humu.20075
4. Elden AC, Kim HJ, Hart MP, Chen-Plotkin AS et al (2010) Ataxin-2 intermediate-length polyglutamine expansions are associated with increased risk for ALS. Nature 466(7310):1069–1075. https://doi.org/10.1038/nature09320
5. Fernandez M, McClain ME, Martinez RA, Snow K et al (2000) Late-onset SCA2: 33 CAG repeats are sufficient to cause disease. Neurology 55(4):569–572. https://doi.org/10.1212/wnl.55.4.569
6. Pulst SM, Nechiporuk A, Nechiporuk T, Gispert S et al (1996) Moderate expansion of a normally biallelic trinucleotide repeat in spinocerebellar ataxia type 2. Nat Genet 14(3):269–276. https://doi.org/10.1038/ng1196-269
7. Cancel G, Dürr A, Didierjean O, Imbert G et al (1997) Molecular and clinical correlations in spinocerebellar ataxia 2: a study of 32 families. Hum Mol Genet 6(5):709–715. https://doi.org/10.1093/hmg/6.5.709
8. Sánchez-Corona J, Ramirez-Garcia SA, Castañeda-Cisneros G, Gutiérrez-Rubio SA et al (2020) A clinical report of the massive CAG repeat expansion in spinocerebellar ataxia type 2: Severe onset in a Mexican child and review previous cases. Genet Mol Biol 43(3):e20190325. https://doi.org/10.1590/1678-4685-gmb-2019-0325
9. Belal S, Cancel G, Stevanin G, Hentati F et al (1994) Clinical and genetic analysis of a Tunisian family with autosomal dominant cerebellar ataxia type 1 linked to the SCA2 locus. Neurology 44(8):1423–1426. https://doi.org/10.1212/wnl.44.8.1423
10. Dürr A, Smadja D, Cancel G, Lezin A et al (1995) Autosomal dominant cerebellar ataxia type I in Martinique (French West Indies). Clinical and neuropathological analysis of 53 patients from three unrelated SCA2 families. Brain 118(Pt 6):1573–1581. https://doi.org/10.1093/brain/118.6.1573
11. Dürr A, Brice A, Lepage-Lezin A, Cancel G et al (1995) Autosomal dominant cerebellar ataxia type I linked to chromosome 12q (SCA2: spinocerebellar ataxia type 2). Clin Neurosci 3(1):12–16
12. Bürk K, Abele M, Fetter M, Dichgans J et al (1996) Autosomal dominant cerebellar ataxia type I clinical features and MRI in

families with SCA1, SCA2 and SCA3. Brain 119(Pt 5):1497–1505. https://doi.org/10.1093/brain/119.5.1497
13. Orozco Diaz G, Nodarse Fleites A, Cordovés Sagaz R, Auburger G (1990) Autosomal dominant cerebellar ataxia: clinical analysis of 263 patients from a homogeneous population in Holguín Cuba. Neurology 40(9):1369–1375. https://doi.org/10.1212/wnl.40.9.1369
14. Filla A, De Michele G, Santoro L, Calabrese O et al (1999) Spinocerebellar ataxia type 2 in southern Italy: a clinical and molecular study of 30 families. J Neurol 246(6):467–471. https://doi.org/10.1007/s004150050385
15. Klockgether T, Lüdtke R, Kramer B, Abele M et al (1998) The natural history of degenerative ataxia: a retrospective study in 466 patients. Brain 121(Pt 4):589–600. https://doi.org/10.1093/brain/121.4.589
16. Magaña JJ, Velázquez-Pérez L, Cisneros B (2013) Spinocerebellar ataxia type 2: clinical presentation, molecular mechanisms, and therapeutic perspectives. Mol Neurobiol 47(1):90–104. https://doi.org/10.1007/s12035-012-8348-8
17. Schöls L, Gispert S, Vorgerd M, Menezes Vieira-Saecker AM et al (1997) Spinocerebellar ataxia type 2. Genotype and phenotype in German kindreds. Arch Neurol 54(9):1073–1080. https://doi.org/10.1001/archneur.1997.00550210011007
18. Estrada R, Galarraga J, Orozco G, Nodarse A et al (1999) Spinocerebellar ataxia 2 (SCA2): morphometric analyses in 11 autopsies. Acta Neuropathol 97(3):306–310. https://doi.org/10.1007/s004010050989
19. Wadia N, Pang J, Desai J, Mankodi A et al (1998) A clinicogenetic analysis of six Indian spinocerebellar ataxia (SCA2) pedigrees. The significance of slow saccades in diagnosis. Brain 121(Pt 12):2341–2355. https://doi.org/10.1093/brain/121.12.2341
20. Orozco G, Estrada R, Perry TL, Araña J et al (1989) Dominantly inherited olivopontocerebellar atrophy from eastern Cuba. Clinical, neuropathological, and biochemical findings. J Neurol Sci 93(1):37–50. https://doi.org/10.1016/0022-510x(89)90159-7
21. Giunti P, Sabbadini G, Sweeney MG, Davis MB et al (1998) The role of the SCA2 trinucleotide repeat expansion in 89 autosomal dominant cerebellar ataxia families. Frequency, clinical and genetic correlates. Brain 121(Pt 3):459–467. https://doi.org/10.1093/brain/121.3.459
22. Imbert G, Saudou F, Yvert G, Devys D et al (1996) Cloning of the gene for spinocerebellar ataxia 2 reveals a locus with high sensitivity to expanded CAG/glutamine repeats. Nat Genet 14(3):285–291. https://doi.org/10.1038/ng1196-285
23. Seidel K, Siswanto S, Fredrich M, Bouzrou M et al (2017) On the distribution of intranuclear and cytoplasmic aggregates in the brainstem of patients with spinocerebellar ataxia type 2 and 3. Brain Pathol 27(3):345–355. https://doi.org/10.1111/bpa.12412
24. Huynh DP, Figueroa K, Hoang N, Pulst SM (2000) Nuclear localization or inclusion body formation of ataxin-2 are not necessary for SCA2 pathogenesis in mouse or human. Nat Genet 26(1):44–50. https://doi.org/10.1038/79162
25. Albrecht M, Golatta M, Wüllner U, Lengauer T (2004) Structural and functional analysis of ataxin-2 and ataxin-3. Eur J Biochem 271(15):3155–3170. https://doi.org/10.1111/j.1432-1033.2004.04245.x
26. van de Loo S, Eich F, Nonis D, Auburger G et al (2009) Ataxin-2 associates with rough endoplasmic reticulum. Exp Neurol 215(1):110–118. https://doi.org/10.1016/j.expneurol.2008.09.020
27. Ralser M, Albrecht M, Nonhoff U, Lengauer T et al (2005) An integrative approach to gain insights into the cellular function of human ataxin-2. J Mol Biol 346(1):203–214. https://doi.org/10.1016/j.jmb.2004.11.024
28. Shibata H, Huynh DP, Pulst SM (2000) A novel protein with RNA-binding motifs interacts with ataxin-2. Hum Mol Genet 9(9):1303–1313. https://doi.org/10.1093/hmg/9.9.1303
29. Bravo J, Aguilar-Henonin L, Olmedo G, Guzmán P (2005) Four distinct classes of proteins as interaction partners of the PABC domain of Arabidopsis thaliana Poly(A)-binding proteins. Mol Genet Genomics 272(6):651–665. https://doi.org/10.1007/s00438-004-1090-9
30. Nonhoff U, Ralser M, Welzel F, Piccini I et al (2007) Ataxin-2 interacts with the DEAD/H-box RNA helicase DDX6 and interferes with P-bodies and stress granules. Mol Biol Cell 18(4):1385–1396. https://doi.org/10.1091/mbc.e06-12-1120
31. Freund HJ, Barnikol UB, Nolte D, Treuer H et al (2007) Subthalamic-thalamic DBS in a case with spinocerebellar ataxia type 2 and severe tremor-a unusual clinical benefit. Mov Disord 22(5):732–735. https://doi.org/10.1002/mds.21338
32. Schmitz-Hübsch T, du Montcel ST, Baliko L, Berciano J et al (2006) Scale for the assessment and rating of ataxia: development of a new clinical scale. Neurology 66(11):1717–1720. https://doi.org/10.1212/01.wnl.0000219042.60538.92
33. Yuan A, Nixon RA (2021) Neurofilament proteins as biomarkers to monitor neurological diseases and the efficacy of therapies. Front Neurosci 15:689938. https://doi.org/10.3389/fnins.2021.689938
34. Wilke C, Bender F, Hayer SN, Brockmann K et al (2018) Serum neurofilament light is increased in multiple system atrophy of cerebellar type and in repeat-expansion spinocerebellar ataxias: a pilot study. J Neurol 265(7):1618–1624. https://doi.org/10.1007/s00415-018-8893-9
35. Coarelli G, Darios F, Petit E, Dorgham K et al (2021) Plasma neurofilament light chain predicts cerebellar atrophy and clinical progression in spinocerebellar ataxia. Neurobiol Dis 153:105311. https://doi.org/10.1016/j.nbd.2021.105311
36. Yang L, Shao YR, Li XY, Ma Y et al (2021) Association of the level of neurofilament light with disease severity in patients with spinocerebellar ataxia type 2. Neurology 97(24):e2404–e2413. https://doi.org/10.1212/wnl.0000000000012945
37. Brouillette AM, Öz G, Gomez CM (2015) Cerebrospinal fluid biomarkers in spinocerebellar ataxia: a pilot study. Dis Markers 2015:413098. https://doi.org/10.1155/2015/413098
38. Jung BC, Choi SI, Du AX, Cuzzocreo JL et al (2012) MRI shows a region-specific pattern of atrophy in spinocerebellar ataxia type 2. Cerebellum 11(1):272–279. https://doi.org/10.1007/s12311-011-0308-8
39. Rüb U, Schöls L, Paulson H, Auburger G et al (2013) Clinical features, neurogenetics and neuropathology of the polyglutamine spinocerebellar ataxias type 1, 2, 3, 6 and 7. Prog Neurobiol 104:38–66. https://doi.org/10.1016/j.pneurobio.2013.01.001
40. Nigri A, Sarro L, Mongelli A, Pinardi C et al (2020) Progression of cerebellar atrophy in spinocerebellar ataxia type 2 gene carriers: a longitudinal MRI study in preclinical and early disease stages. Front Neurol 11:616419. https://doi.org/10.3389/fneur.2020.616419
41. Weiss A, Abramowski D, Bibel M, Bodner R et al (2009) Single-step detection of mutant huntingtin in animal and human tissues: a bioassay for Huntington's disease. Anal Biochem 395(1):8–15. https://doi.org/10.1016/j.ab.2009.08.001
42. Weiss A, Träger U, Wild EJ, Grueninger S et al (2012) Mutant huntingtin fragmentation in immune cells tracks Huntington's disease progression. J Clin Invest 122(10):3731–3736. https://doi.org/10.1172/jci64565
43. Baldo B, Paganetti P, Grueninger S, Marcellin D et al (2012) TR-FRET-based duplex immunoassay reveals an inverse correlation of soluble and aggregated mutant huntingtin in huntington's disease. Chem Biol 19(2):264–275. https://doi.org/10.1016/j.chembiol.2011.12.020
44. Nguyen HP, Hübener J, Weber JJ, Grueninger S et al (2013) Cerebellar soluble mutant ataxin-3 level decreases during disease

progression in spinocerebellar ataxia type 3 mice. PLoS One 8(4):e62043. https://doi.org/10.1371/journal.pone.0062043
45. Gonsior K, Kaucher GA, Pelz P, Schumann D et al (2021) PolyQ-expanded ataxin-3 protein levels in peripheral blood mononuclear cells correlate with clinical parameters in SCA3: a pilot study. J Neurol 268(4):1304–1315. https://doi.org/10.1007/s00415-020-10274-y
46. Wild EJ, Boggio R, Langbehn D, Robertson N et al (2015) Quantification of mutant huntingtin protein in cerebrospinal fluid from Huntington's disease patients. J Clin Invest 125(5):1979–1986. https://doi.org/10.1172/jci80743
47. Hübener-Schmid J, Kuhlbrodt K, Peladan J, Faber J et al (2021) Polyglutamine-expanded ataxin-3: a target engagement marker for spinocerebellar ataxia type 3 in peripheral blood. Mov Disord 36(11):2675. https://doi.org/10.1002/mds.28749
48. Laffita-Mesa JM, Paucar M, Svenningsson P (2021) Ataxin-2 gene: a powerful modulator of neurological disorders. Curr Opin Neurol 34(4):578. https://doi.org/10.1097/wco.0000000000000959
49. Raposo M, Ramos A, Bettencourt C, Lima M (2015) Replicating studies of genetic modifiers in spinocerebellar ataxia type 3: can homogeneous cohorts aid? Brain 138(Pt 12):e398. https://doi.org/10.1093/brain/awv206
50. Santos D, Coelho T, Alves-Ferreira M, Sequeiros J et al (2019) Large normal alleles of ATXN2 decrease age at onset in transthyretin familial amyloid polyneuropathy Val30Met patients. Ann Neurol 85(2):251–258. https://doi.org/10.1002/ana.25409
51. Rubino E, Mancini C, Boschi S, Ferrero P et al (2019) ATXN2 intermediate repeat expansions influence the clinical phenotype in frontotemporal dementia. Neurobiol Aging 73:231.e7–231.e9. https://doi.org/10.1016/j.neurobiolaging.2018.09.009
52. Rosas I, Martínez C, Clarimón J, Lleó A et al (2020) Role for ATXN1, ATXN2, and HTT intermediate repeats in frontotemporal dementia and Alzheimer's disease. Neurobiol Aging 87:139.e1–139.e7. https://doi.org/10.1016/j.neurobiolaging.2019.10.017
53. Glass JD, Dewan R, Ding J, Gibbs JR et al (2022) ATXN2 intermediate expansions in amyotrophic lateral sclerosis. Brain. 145(8):2671–2676. https://doi.org/10.1093/brain/awac167
54. Sellier C, Campanari ML, Julie Corbier C, Gaucherot A et al (2016) Loss of C9ORF72 impairs autophagy and synergizes with polyQ Ataxin-2 to induce motor neuron dysfunction and cell death. Embo J 35(12):1276–1297. https://doi.org/10.15252/embj.201593350
55. Wang MD, Gomes J, Cashman NR, Little J et al (2014) Intermediate CAG repeat expansion in the ATXN2 gene is a unique genetic risk factor for ALS--a systematic review and meta-analysis of observational studies. PLoS One 9(8):e105534. https://doi.org/10.1371/journal.pone.0105534
56. Fournier C, Anquetil V, Camuzat A, Stirati-Buron S et al (2018) Interrupted CAG expansions in ATXN2 gene expand the genetic spectrum of frontotemporal dementias. Acta Neuropathol Commun 6(1):41. https://doi.org/10.1186/s40478-018-0547-8
57. Laffita-Mesa JM, Nennesmo I, Paucar M, Svenningsson P (2021) A novel duplication in ATXN2 as modifier for spinocerebellar ataxia 3 (SCA3) and C9ORF72-ALS. Mov Disord 36(2):508–514. https://doi.org/10.1002/mds.28334
58. Damrath E, Heck MV, Gispert S, Azizov M et al (2012) ATXN2-CAG42 sequesters PABPC1 into insolubility and induces FBXW8 in cerebellum of old ataxic knock-in mice. PLoS Genet 8(8):e1002920. https://doi.org/10.1371/journal.pgen.1002920
59. Sen NE, Canet-Pons J, Halbach MV, Arsovic A et al (2019) Generation of an Atxn2-CAG100 knock-in mouse reveals N-acetylaspartate production deficit due to early Nat8l dysregulation. Neurobiol Dis 132:104559. https://doi.org/10.1016/j.nbd.2019.104559
60. Hauser S, Höflinger P, Theurer Y, Rattay TW et al (2016) Generation of induced pluripotent stem cells (iPSCs) from a hereditary spastic paraplegia patient carrying a homozygous Y275X mutation in CYP7B1 (SPG5). Stem Cell Res 17(2):437–440. https://doi.org/10.1016/j.scr.2016.09.011
61. Hauser S, Schuster S, Heuten E, Höflinger P et al (2020) Comparative transcriptional profiling of motor neuron disorder-associated genes in various human cell culture models. Front Cell Dev Biol 8:544043. https://doi.org/10.3389/fcell.2020.544043
62. Bradford MM (1976) A rapid and sensitive method for the quantitation of microgram quantities of protein utilizing the principle of protein-dye binding. Anal Biochem 72:248–254. https://doi.org/10.1006/abio.1976.9999
63. Laemmli UK (1970) Cleavage of structural proteins during the assembly of the head of bacteriophage T4. Nature 227(5259):680–685. https://doi.org/10.1038/227680a0
64. Burnette WN (1981) "Western blotting": electrophoretic transfer of proteins from sodium dodecyl sulfate--polyacrylamide gels to unmodified nitrocellulose and radiographic detection with antibody and radioiodinated protein A. Anal Biochem 112(2):195–203. https://doi.org/10.1016/0003-2697(81)90281-5
65. Wilke C, Haas E, Reetz K, Faber J et al (2020) Neurofilaments in spinocerebellar ataxia type 3: blood biomarkers at the preataxic and ataxic stage in humans and mice. EMBO Mol Med 12(7):e11803. https://doi.org/10.15252/emmm.201911803
66. Xia H, Mao Q, Eliason SL, Harper SQ et al (2004) RNAi suppresses polyglutamine-induced neurodegeneration in a model of spinocerebellar ataxia. Nat Med 10(8):816–820. https://doi.org/10.1038/nm1076
67. Friedrich J, Kordasiewicz HB, O'Callaghan B, Handler HP et al (2018) Antisense oligonucleotide-mediated ataxin-1 reduction prolongs survival in SCA1 mice and reveals disease-associated transcriptome profiles. JCI. Insight 3(21). https://doi.org/10.1172/jci.insight.123193
68. Scoles DR, Meera P, Schneider MD, Paul S et al (2017) Antisense oligonucleotide therapy for spinocerebellar ataxia type 2. Nature 544(7650):362–366. https://doi.org/10.1038/nature22044
69. Kordasiewicz HB, Stanek LM, Wancewicz EV, Mazur C et al (2012) Sustained therapeutic reversal of Huntington's disease by transient repression of huntingtin synthesis. Neuron 74(6):1031–1044. https://doi.org/10.1016/j.neuron.2012.05.009
70. Evers MM, Tran HD, Zalachoras I, Meijer OC et al (2014) Preventing formation of toxic N-terminal huntingtin fragments through antisense oligonucleotide-mediated protein modification. Nucleic Acid Ther 24(1):4–12. https://doi.org/10.1089/nat.2013.0452
71. Martier R, Sogorb-Gonzalez M, Stricker-Shaver J, Hübener-Schmid J et al (2019) Development of an AAV-based microRNA gene therapy to treat Machado-Joseph disease. Mol Ther Methods Clin Dev 15:343–358. https://doi.org/10.1016/j.omtm.2019.10.008
72. Moore LR, Rajpal G, Dillingham IT, Qutob M et al (2017) Evaluation of antisense oligonucleotides targeting ATXN3 in SCA3 mouse models. Mol Ther Nucleic Acids 7:200–210. https://doi.org/10.1016/j.omtn.2017.04.005
73. Evers MM, Tran HD, Zalachoras I, Pepers BA et al (2013) Ataxin-3 protein modification as a treatment strategy for spinocerebellar ataxia type 3: removal of the CAG containing exon. Neurobiol Dis 58:49–56. https://doi.org/10.1016/j.nbd.2013.04.019
74. Hauser S, Helm J, Kraft M, Korneck M et al (2022) Allele-specific targeting of mutant ataxin-3 by antisense oligonucleotides in SCA3-iPSC-derived neurons. Mol Ther Nucleic Acids 27:99–108. https://doi.org/10.1016/j.omtn.2021.11.015
75. Klein FA, Zeder-Lutz G, Cousido-Siah A, Mitschler A et al (2013) Linear and extended: a common polyglutamine conformation

recognized by the three antibodies MW1, 1C2 and 3B5H10. Hum Mol Genet 22(20):4215–4223. https://doi.org/10.1093/hmg/ddt273
76. Klockgether T, Mariotti C, Paulson HL (2019) Spinocerebellar ataxia. Nat Rev Dis Primers 5(1):24. https://doi.org/10.1038/s41572-019-0074-3
77. Lonsdale J, Thomas J, Salvatore M, Phillips R, Lo E, Shad S, Hasz R, Walters G et al (2013) The Genotype-Tissue Expression (GTEx) project. Nat Genet 45(6):580–585. https://doi.org/10.1038/ng.2653
78. Lastres-Becker I, Nonis D, Eich F, Klinkenberg M et al (1862) (2016) Mammalian ataxin-2 modulates translation control at the pre-initiation complex via PI3K/mTOR and is induced by starvation. Biochim Biophys Acta 9:1558–1569. https://doi.org/10.1016/j.bbadis.2016.05.017
79. Bidinosti M, Shimshek DR, Mollenhauer B, Marcellin D et al (2012) Novel one-step immunoassays to quantify α-synuclein: applications for biomarker development and high-throughput screening. J Biol Chem 287(40):33691–33705. https://doi.org/10.1074/jbc.M112.379792
80. Scoles DR, Ho MH, Dansithong W, Pflieger LT et al (2015) Repeat associated non-AUG translation (RAN translation) dependent on sequence downstream of the ATXN2 CAG Repeat. PLoS One 10(6):e0128769. https://doi.org/10.1371/journal.pone.0128769
81. Asada A, Yamazaki R, Kino Y, Saito T et al (2014) Cyclin-dependent kinase 5 phosphorylates and induces the degradation of ataxin-2. Neurosci Lett 563:112–117. https://doi.org/10.1016/j.neulet.2014.01.046
82. Lastres-Becker I, Nonis D, Nowock J, Auburger G (2019) New alternative splicing variants of the ATXN2 transcript. Neurol Res Pract 1:22. https://doi.org/10.1186/s42466-019-0025-1
83. Inada R, Hirano M, Oka N, Samukawa M et al (2021) Phenotypic and molecular diversities of spinocerebellar ataxia type 2 in Japan. J Neurol 268(8):2933–2942. https://doi.org/10.1007/s00415-021-10467-z